PNAS
www.pnas.org

Supplementary Information for

NAD$^+$ supplementation reduces neuroinflammation and cell senescence in a transgenic mouse model of Alzheimer's disease via cGAS-STING

Yujun Hou, Yong Wei, Sofie Lautrup, Beimeng Yang, Yue Wang, Stephanie Cordonnier, Mark P. Mattson, Deborah L. Croteau, and Vilhelm A. Bohr

Corresponding author: Vilhelm A. Bohr
Email: vbohr@nih.gov

This PDF file includes:

Supplementary Information Text

Materials and Methods

Morris water maze and Y-maze. The Morris water maze (MWM) test was performed as previously described (1-3). Briefly, the equipment is a circular pool (140 cm in diameter), and the water is kept at 22˚C. A transparent 12-cm diameter platform was placed at a fixed position 1 cm below the water surface. Mice were trained for 7 consecutive days, with 4 trials/day. Each trial lasted 60 s or until the mouse found the hidden platform. On the 8th day, the 60 sec probe trial was performed after the platform was removed. The Y Maze Spontaneous Alternation Performance (SAP) test was performed as previous reported (4, 5).

Open field, rotarod and grip strength test. For the open field test, animals were placed in the center of a defined open field region (43 cm × 43 cm) (Med Associates, Georgia, VT, USA) and left without disruption for 30 min. The center zone was defined as a 10.2 cm^2 equidistant from the peripheral walls. The tracking software (Activity monitor version 4, Med-Associates) recorded the exploratory behavior. The apparatus was cleaned with 70% ethanol before testing the next mouse. For the rotarod test, mice were placed onto the ENV-577M Rotarod system (Med Associates, Georgia) at a walking speed of 4 rpm. Then, the speed was increased to 40 rpm in 300 seconds. Latency for the animal to fall off the rotarod was recorded (6). For the grip strength test, each individual's forelimbs were tested for grip strength by pulling on a wire attached to a Chatillon DFE-002 force gauge (Chatillon Force Measurement Systems). Five pulls were performed for each mouse. The mean of the recordings was determined.

NAD$^+$ detection. As described in a previous report (2), mouse cerebral cortex samples were collected and lysed, and NAD$^+$, NADH and NAD$^+$/NADH ratios were measured by using the NAD$^+$/NADH assay kit (Abcam, #ab65348) according to the manufacturer's protocol.

Microarray. Gene expression analysis was performed on the brain hippocampus and cortex tissues of NR- or vehicle- treated APP/PS1 and WT mice. n = 6 WT, 6 WT(NR), 7 AD, 5 AD(NR) mice for analysis. RNA was purified and inspected as reported previously (3, 5, 7). The entire set was tested using parametric analysis of gene set enrichment (PAGE) for Geneset enrichment. Detailed data analysis was performed using our previously reported protocols (2, 3, 8). For each pairwise comparison a pathway aggregation z-score was obtained from the gene-expression change z-ratio, and a *t* test *P* value to the whole array genes and FDR was computed using PAGE analysis software to test for the significance of the z-score obtained. Pathways per gene set were considered significant if they had more than three genes found in the array and a *t* test *P* value of less than 0.05 with an FDR of not more than 0.05. The gene expression data has been deposited with GEO (GSE135999).

Electrophysiology. Hippocampal slices were prepared as described (2, 9). And the electrophysiology was performed as we reported previously (2).

Immunofluorescence. The immunofluorescence staining was performed in mouse brain sections and cells as we reported previously (3). Pictures were taken using an Axiovert 200M Zeiss microscope (Zeiss) or a Zeiss 710 LSM confocal microscope (Zeiss). Images were quantified using ImageJ 1.52p. Specific primary antibodies used include rabbit anti-GFAP (DAKO, #Z033401-2), mouse anti-6E10 for Aβ (BioLegend, #803002), goat anti-IBA1 (NOVUS, #NB100-1028), rabbit anti-IBA1 (WAKO, #019-19741), NLRP3 (Adipogen, #AG-20B-0014-C100), Caspase-1 (AdipoGen, #AG-20B-0042-C100), γH2AX (Cell Signaling, #9719), cleaved-Caspase-3 (Cell signaling, #9759S), ssDNA (Sigma, #MAB3299), dsDNA (Sigma, #MAB1293), TOMM20 (Proteintech, #11802-1-AP), LAMP2 (Proteintech, 66301-1-Ig), NeuN (Sigma, #MAB377), Olig2 (IBL-America, #18953), p16^{INK4a} (abcam, #211542), p21 (abcam, #188224), p21 (Proteintech, #27296-1-AP) antibodies. The numbers of specific cells per mm^2 were counted using ImageJ. To stain ssDNA and dsDNA, we followed the instructions. Microglia stained with IBA1 were evaluated for morphological changes by measuring the average process length (10). To evaluate the phagocytosis of microglia, we used = (number of microglia with Aβ plaques per ROI)/(total number of microglia per ROI).

Mitophagy was measured using the mitophagy detection kit (Dojindo, #MD01-10) according to the manufacturer's protocol.

Western Blots. Western blot analyses were performed as described previously (3). Gamma adjustment was used to reduce the dark background when necessary. Quantification was performed using ImageJ. Antibodies used were: NLRP3 (Adipogen, #AG-20B-0014-C100), AIM2 (Cell Signaling, #63660), NLRP1 (NOVUS, #NBP1-54899), NLRC4 (NOVUS, #NB100-56142), Caspase-1 (Proteintech, #22915-1-AP), IL-1β (Proteintech, #10806-1-AP), p65 (Proteintech, #10745-1-AP), IFN-γ (Proteintech, #15365-1-AP), IL-18 (Proteintech, #10663-1-AP), cGAS (Cell Signaling, #31659 and #15102), STING (Cell Signaling, #13647), CSF2RA (R&D, #MAB6130-100), Osteopontin (Abcam, #ab8448), γH2AX (Cell signaling, #9718), pAMPK (Thr172) (Cell Signaling, #2535), AMPK (Cell Signaling, #5831), p-ULK1 (Ser555) (Cell Signaling, #5869), ULK1 (Cell Signaling, #6439), p62 (Sigma, #P0067), LC3 (Novus, #NB100-2220) and β-actin (Santa Cruz Biotechnology, #sc-1616; Cell signaling, #4970).

Cell culture. HMC3 human microglia cells were previously purchased from ATCC (#CRL0314). Cell lines were cultured in Eagle's Minimum Essential Medium with 10% (w/v) fetal bovine serum in a humidified incubator with 5% CO2/95% air (v/v) at 37°C. Primary AD fibroblasts (AG07374) and age-matched control fibroblasts (AG09857) were purchased from Corriell Institute for Medical Research. They were grown in AmnioMAX II Complete Medium (no. 11269016; Gibco) and were protected from light. Cells were in passages 3–7 for experiments. Mouse primary microglia from C57BL/6 were purchased from ScienCell (#M1900-57) and cultured in microglia medium (ScienCell, #1901).

ELISA for cytokines. The HMC3 cell and primary microglia supernatants were analyzed by ELISA. Human IL-6 was measured by IL-6 kit (R&D systems, #D6050). Mouse ELISA kits for cytokines were purchased from R&D systems: IL-6 (#M6000B), IL-1β (#MLB00C) and TNFα (#MTA00B). STING inhibitor H-151 was purchased from MCE (#HY-112693), the final concentration was 1 μM. The siRNAs were from Dharmacon: human si-cGAS (#E-015607-00-0005), human si-STING (#E-024333-00-0005), mouse si-cGAS (#E-055608-00-0010), mouse si-STING (#E-55528-00-0010), si-PINK1 (#E-004030-00-0005), si-ULK1 (#E-005049-00-0005), si-BNIP3L/NIX (#E-011815-00-0005).

Preparation of Aβ peptides. The peptides were prepared according to the protocols described previously. Briefly, hexafluoroisopropanol (HFIP)-treated $A\beta_{42}$ peptides (Abcam) were resuspended in DMSO, then diluted to a concentration of 100 μM with PBS and incubated at 4˚C for 24 hours. After centrifugation 10 min at 14,000 g, the supernatant with soluble $A\beta_{42}$ was added to cultures.

Cytokine array. For mouse brain lysates, tissues were lysed and centrifuged, and the supernatant was flash frozen until cytokine array did (not diluted). Mouse eye bleeds were collected in EDTA-treated tubes. After centrifugation, the supernatant was flash frozen. 1:2 diluted plasma was used to detect cytokines and chemokines by use of 31-Plex Cytokine/Chemokine array (Eve Technologies).

SA-β-gal staining. Staining for SA-β-gal was performed on free-floating mouse brain sections in the SA-β-gal staining solution (Cell Signaling Technology, #9860) at 37°C for 24 h. HMC3 cells were stained in the same SA-β-gal staining solution at 37°C for 24 h following the instruction.

RNA extraction and quantitative real-time PCR. RNA was extracted from mouse or cell samples as reported previously (3). cDNA was synthesized using iScript cDNA Synthesis kit (BioRad) and qPCR analysis was done with power SYBR Green PCR master mix (Thermo Fisher). The primers used to amplify each transcript are as follows: $p16^{INK4a}$ (forward: 5'-AATCTCCGCGAGGAAAGC-3' and reverse: 5'-GTCTGCAGCGGACTCCAT-3'), p21 (forward: 5'-TTGCCAGCAGAATAAAAGGTG-3' and reverse: 5'-TTTGCTCCTGTGCGGAAC-3'), p15 (forward: 5'-AGATCCCAACGCCCTGAAC-3' and reverse: 5'-CCCATCATCATGACCTGGATT-3'), Arg1 (forward: 5'-GGACCTGGCCTTTGTTGATG-3' and reverse: 5'-AGACCGTGGGTTCTTCACAATT-3'), Fizz1 (forward: 5'-CCCTCCACTGTAACGAAGACTC-3' and reverse: 5'-CACACCCAGTAGCAGTCATCC-3'),

YM1 (forward: 5’-CATGAGCAAGACTTGCGTGAC-3’ and reverse: 5’-GGTCCAAACTTCCATCCTCCA-3’).

Subcellular fractionation. Subcellular fractionation and mitochondrial DNA quantification was adapted and modified from Aarreberg et al. (11) as follows: AD human fibroblasts or control human fibroblasts were lysed in MS buffer (225 mM Mannitol, 75 mM Sucrose, 5 mM Hepes, 1 mM EGTA, 0.1% Fatty acid free BSA, pH to 7.4 with KOH) and incubated on a rotator at 4°C. Samples were centrifuged at 2,200xg for 3 min at 4°C. Supernatants were transferred to fresh tubes and centrifuged at 22,000xg for 10 min at 4°C, transferring supernatants to fresh tubes, this constituted the cytosolic fraction. Then resuspended the pellet in 1 ml MS buffer and centrifuged at 22,000xg for 10 min at 4°C, the pellet constituted the mitochondrial fraction. DNA was subsequently extracted from the appropriate cytosolic and mitochondrial fractions using the QIAmp DNA Mini Kit (QIAGEN). Cytosolic and mitochondrial DNA was used for qPCR analysis of mitochondrial DNA using gene-specific primers (11). The primers used to amplify each transcript are as follows: mt-ND1 (forward: 5’-CACCCAAGAACAGGGTTTGT-3’ and reverse: 5’-TGG CCATGGGTATGTTGTTAA-3’), mt-D-LOOP (5’-CTATCACCCTATTAACCACTCA-3’ and reverse: 5’-TTCGCCTGTAATATTGAACGTA-3’), mt-CO2 (5’-AATCGAGTAGTACTCCCGATTG-3’ and reverse: 5’-TTCTAGGACGATGGGCATGAAA-3’), mt-ATP6 (5’-AATCCAAGCCTACGTTTTCACA-3’ and reverse: 5’-AGTATGAGGAGCGTTATGGAGT-3’).

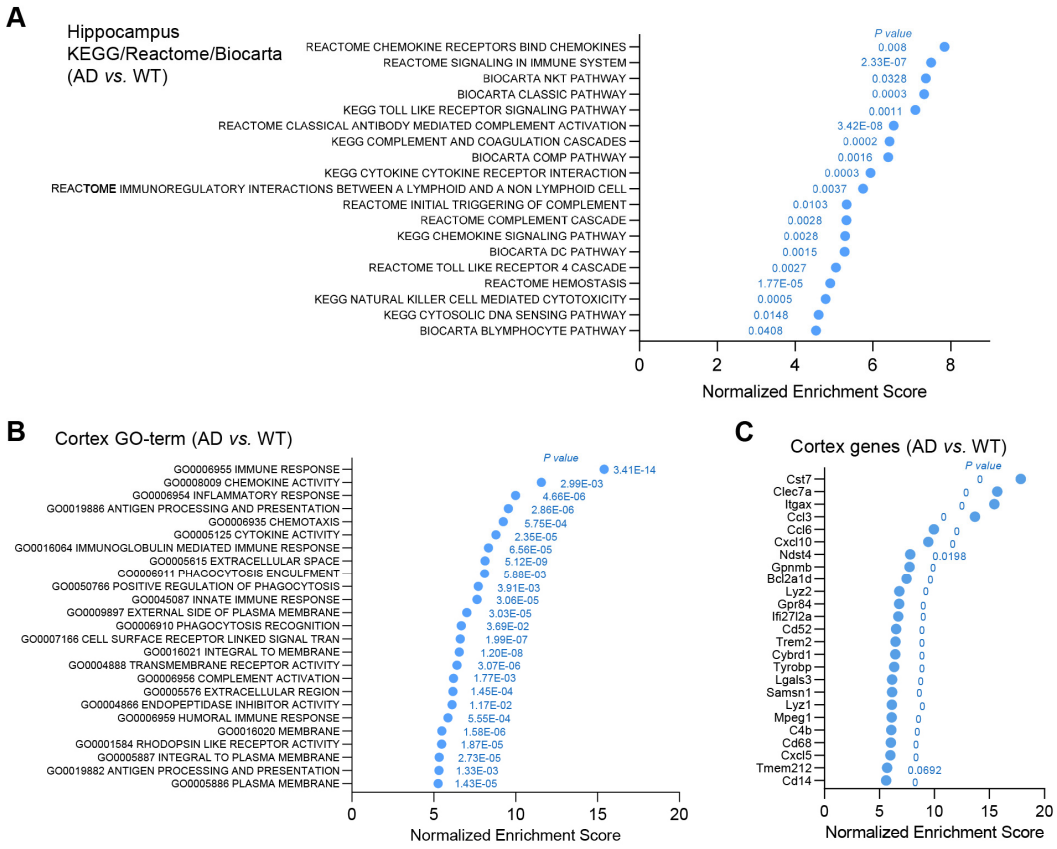

Fig. S1. Several inflammation pathways and genes changed in AD mouse hippocampus and cortex compared to WT.

(**A**) Gene expression analysis using microarray. The normalized enrichment score of KEGG, Reactome or Biocarta most changed pathways in hippocampus of AD mice compared to WT. (**B**) The normalized enrichment score of GO-terms most changed pathways in cortex of AD mice compared to WT. *P* values for each significant changed pathway are shown. (**C**) The most changed genes in cortex of AD compared to WT. *P* values for each significant changed gene are shown.

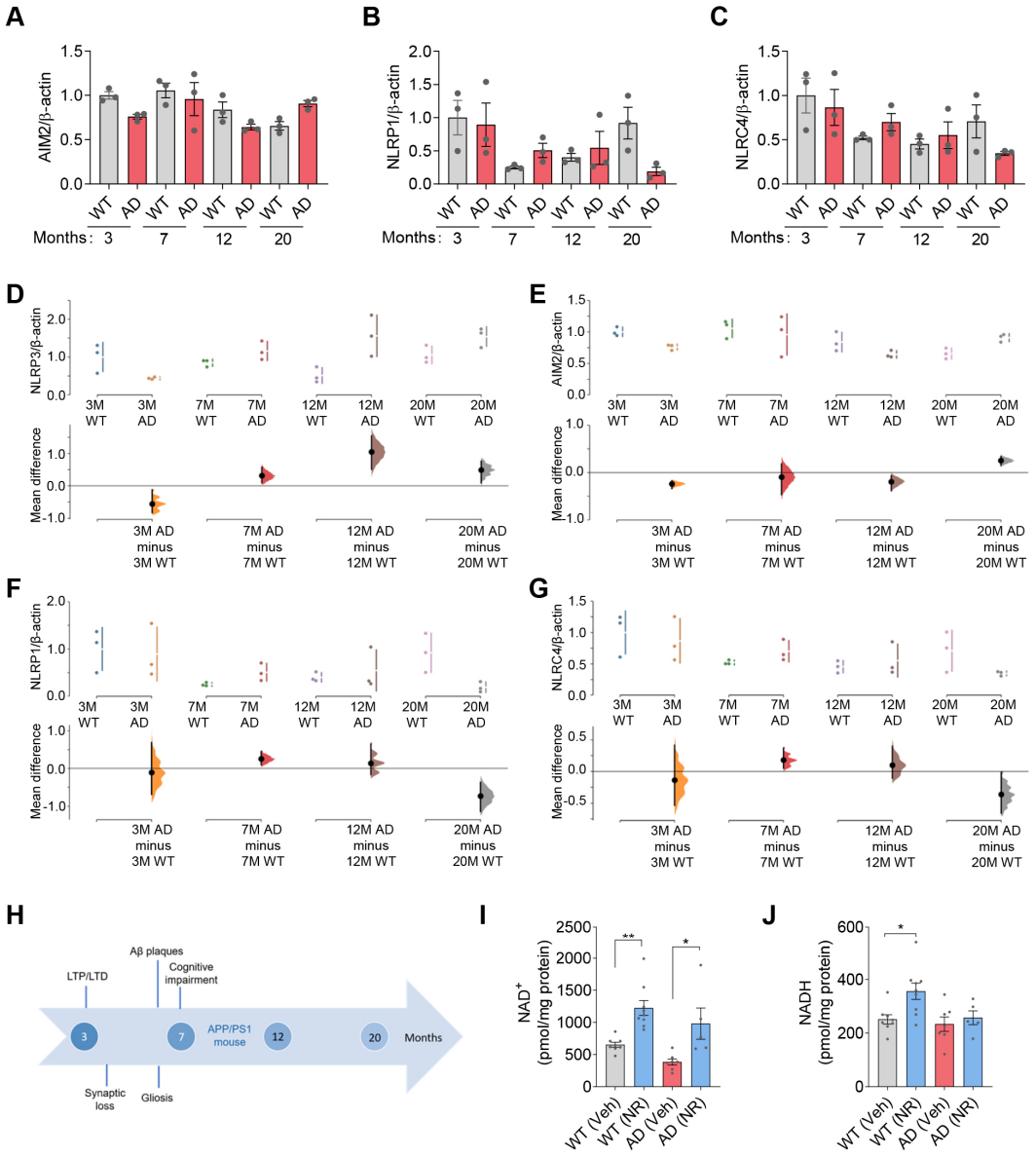

Fig. S2. Comparison of the levels of some Inflammasomes in the cortex of AD and WT mice; After NR treatment, the NAD⁺ levels in the cortex of AD and WT mice increased. (**A**) Quantification of protein AIM2 in Fig. 1C. (**B**) Quantification of protein NLRP1 in Fig. 1C. (**C**) Quantification of protein NLRC4 in Fig. 1C. (**D-G**) Estimation statistics for proteins quantification in Fig. 1C were performed as described in Methods. The raw data was plotted on the upper axes; each mean difference was plotted on the lower axes as a bootstrap sampling distribution. Mean differences were depicted as dots; 95% confidence intervals were indicated by the ends of the vertical error bars. (**H**) Phenotypic characterization of APP/PS1 mice. Aβ deposits can be found by 6 months and increased with age. Gliosis can be seen at 6 months and especially in areas around plaques. Transient long-term potentiation (LTP) is reduced by 3 months. The mice develop cognitive impairment in the brain by 7 months of age, which worsened with age. Refer to Alzforum (https://www.alzforum.org/research-models/appswepsen1de9-line-85) for more information. (**I**) NAD^+ levels in 12-month AD and WT mice cortex with or without NR treatment. n= 5-9 mice per group. (**I**) NADH levels in 12-month AD and WT mice cortex with or without NR treatment. n= 5-9 mice per group. Data: mean ± S.E.M. Statistical significance was performed with Two-way ANOVA followed by Tukey's multiple comparisons test compared with control. * $P < 0.05$, ** $P < 0.01$, *** $P < 0.001$.

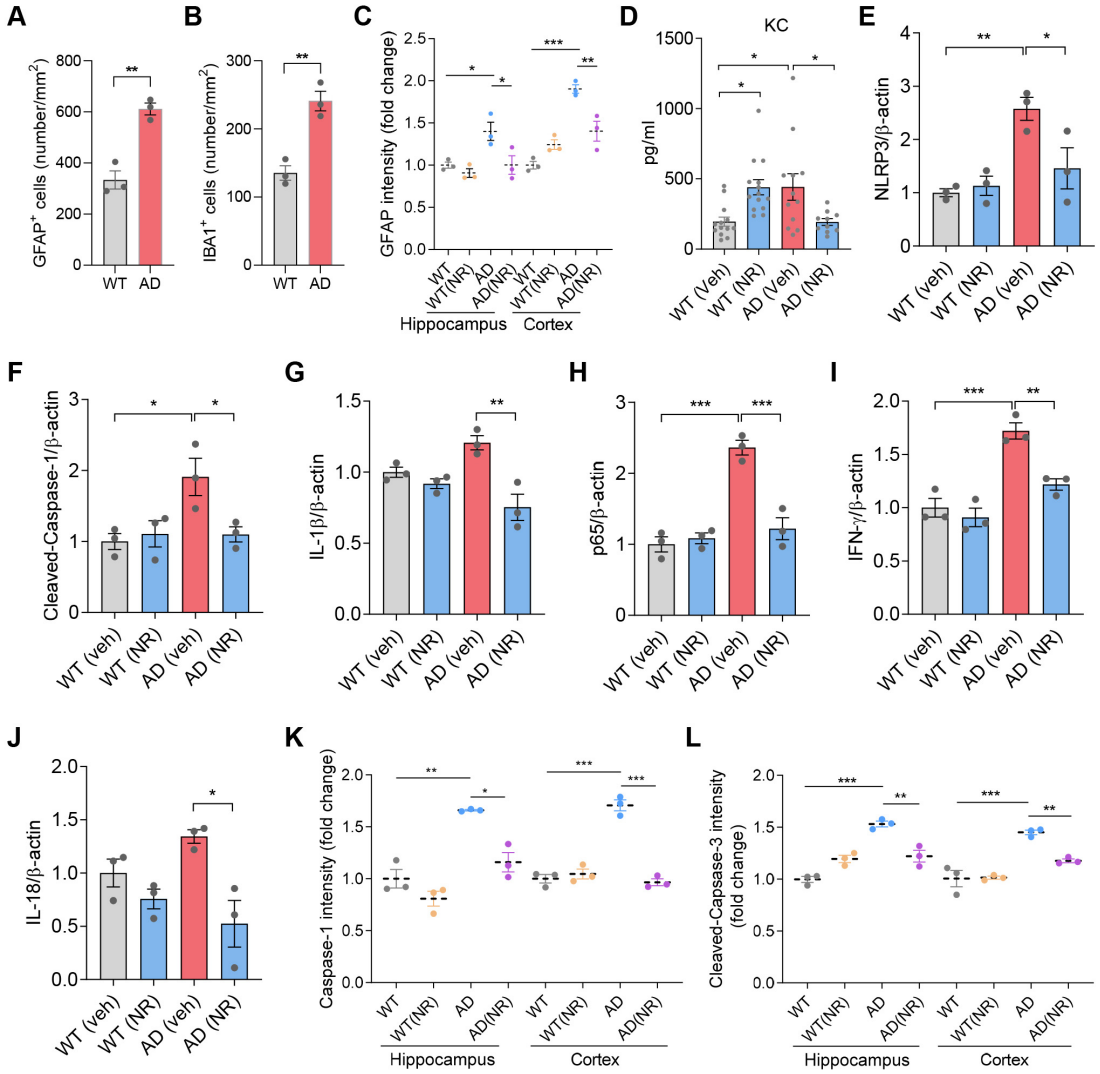

Fig. S3. NR normalizes neuroinflammation and DNA damage in AD mice.
(**A**) The GFAP$^+$ astrocytes number per mm^2 in WT and APP/PS1 AD mouse cortex tissues in Fig. 2A. n = 3 mice per group. (**B**) The IBA1$^+$ microglia number per mm^2 in WT and APP/PS1 AD mouse cortex tissues in Fig. 2A. n = 3 mice per group. (**C**) Quantification of GFAP intensity in Fig. 2A. n = 3 mice per group. (**D**) Pro-inflammatory chemokine KC levels detected by cytokine array in AD or WT mice plasma with or without NR treatment. n = 10~14 mice per group. (**E**) Quantification of NLRP3 protein levels in Fig. 2H. n = 3 mice per group. (**F**) Quantification of cleaved-Caspase-1 protein levels in Fig. 2H. n = 3 mice per group. (**G**) Quantification of IL-1β protein levels in Fig. 2H. n = 3 mice per group. (**H**) Quantification of p65 protein levels in Fig. 2H. n = 3 mice per group. (**I**) Quantification of IFNγ protein levels in Fig. 2H. n = 3 mice per group. (**J**) Quantification of IL-18 protein levels in Fig. 2H. n = 3 mice per group. (**K**) Quantification of Caspase-1 intensity in Fig. 2I. n = 3 mice per group. (**L**) Quantification of cleaved-Caspase-3 intensity in Fig. 2K. n = 3 mice per group. Data: mean ± S.E.M. Statistical significance was performed with Student's *t*-test or Two-way ANOVA followed by Tukey's or Bonferroni multiple comparisons test. * $P < 0.05$, ** $P < 0.01$, *** $P < 0.001$.

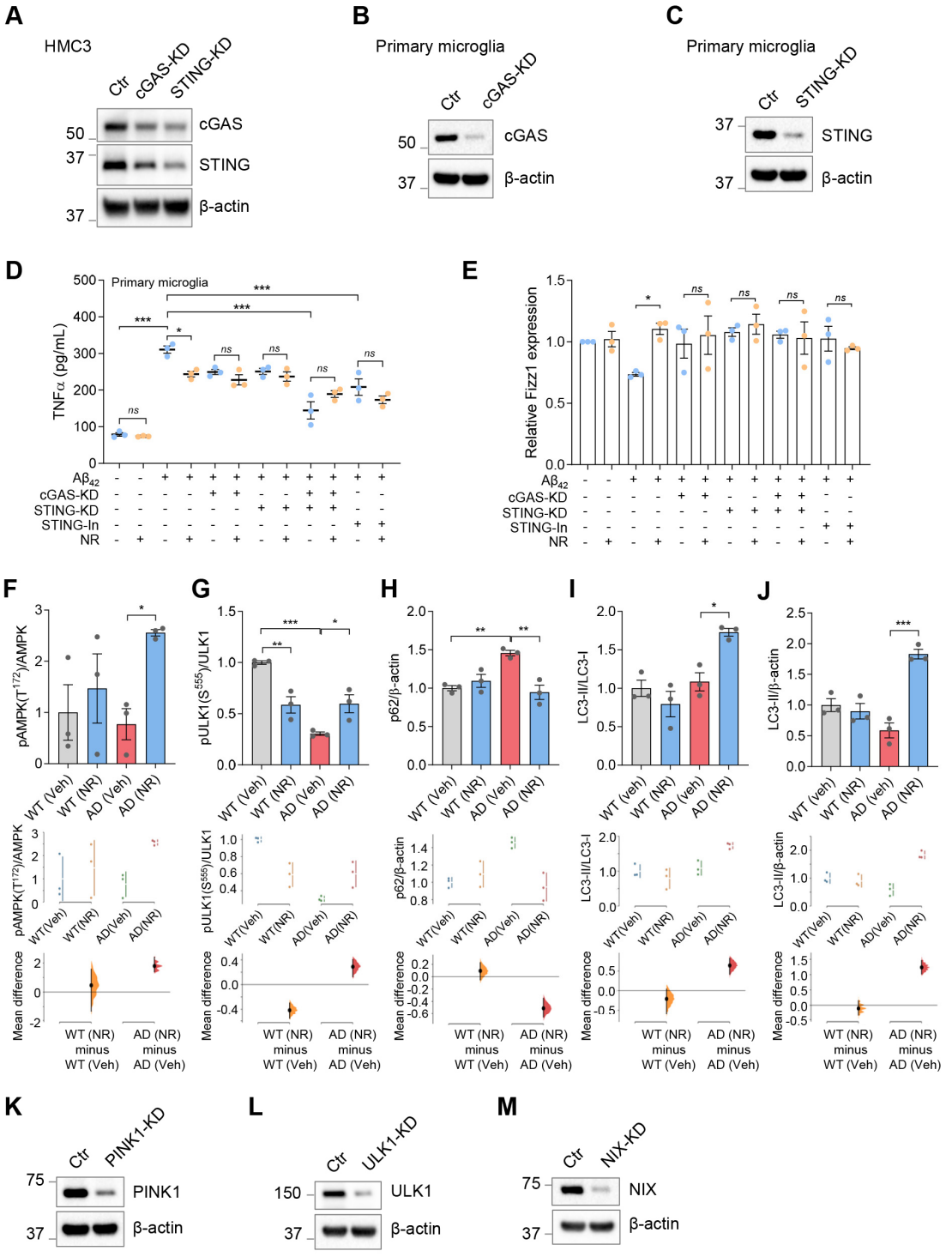

Fig. S4. NR decreases neuroinflammation *in vitro* and induces mitophagy in AD mice. (**A**) Western blots of cGAS or STING proteins in cGAS or STING knockdown (using siRNAs) HMC3 cell. (**B-C**) Western blots of cGAS or STING proteins in cGAS or STING knockdown (using siRNAs) mouse primary microglia cell. (**D**) ELISA of TNFα level in different conditions of mouse primary microglia cell supernatants. Cells were treated by combining $A\beta_{42}$ (5 μM) and/or NR (1 mM) and/or STING inhibitor H151 (1 μM) or cGAS-KD and/or STING-KD for 72 hours. n = 3 biological repeats. (**E**) Quantitative PCR of M2 maker Fizz1 in different conditions of mouse primary microglia cell, same cell setting as Fig. 3H. (**F-J**) Quantification of pAMPK(T^{172})/AMPK, pULK1(S^{555})/ULK1, p62, ratio of LC3-II to LC3-I and LC3-II levels in mice cortex in Fig. 4H. n = 3 mice per group. Lower panels: Estimation statistics for proteins

quantification in Fig. 4H were performed as described in Methods. The raw data was plotted on the middle axes; each mean difference was plotted on the lower axes as a bootstrap sampling distribution. Mean differences were depicted as dots; 95% confidence intervals were indicated by the ends of the vertical error bars. (**K-M**) Western blots of PINK1 or ULK1 or NIX proteins in their knockdown (using siRNAs) human AD fibroblasts. Data: mean ± S.E.M. Statistical significance was performed with one-way or two-way ANOVA followed by Tukey's multiple comparisons test. * $P < 0.05$, ** $P < 0.01$, *** $P < 0.001$.

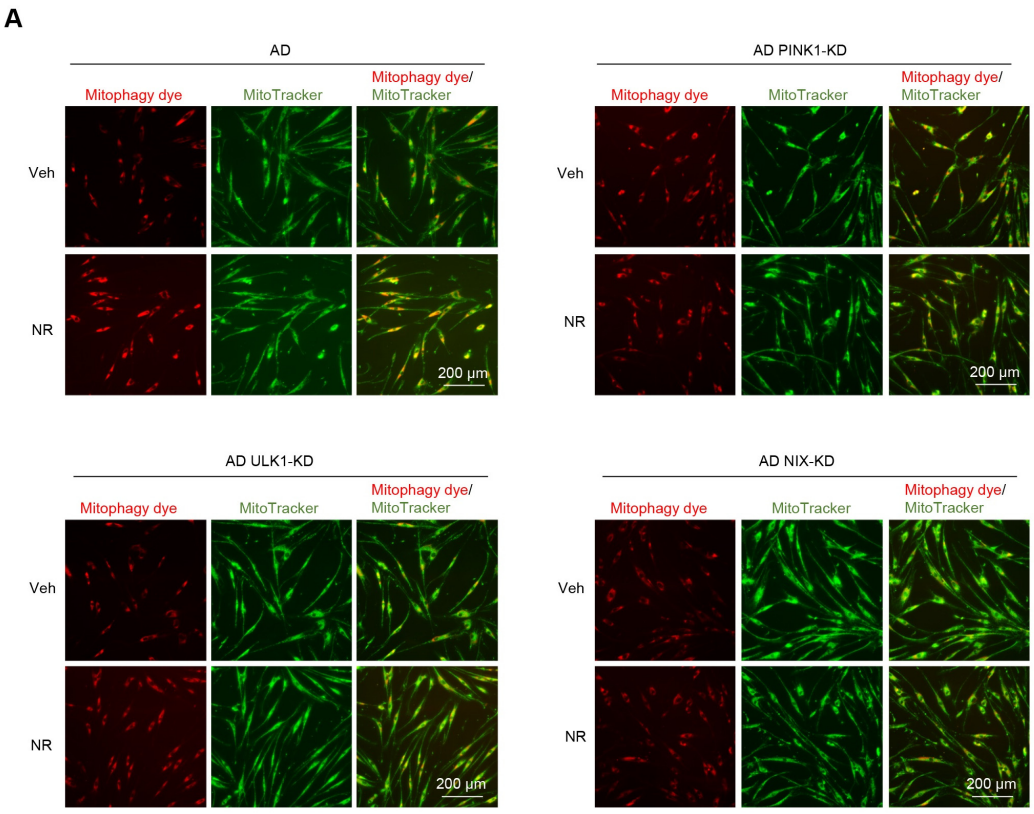

Fig. S5. NR induces mitophagy in human AD fibroblasts.
(**A**) Mitophagy dye and mitochondria marker mitoTracker staining in human AD fibroblasts. We knocked down some mitophagy genes: PINK1, ULK1 or NIX in human AD fibroblasts, which treated with or without 1 mM NR treatment. Mitophagy was measured by using mitophagy detection kit (Dojindo). The quantification of the Figure is in Fig. 4I.

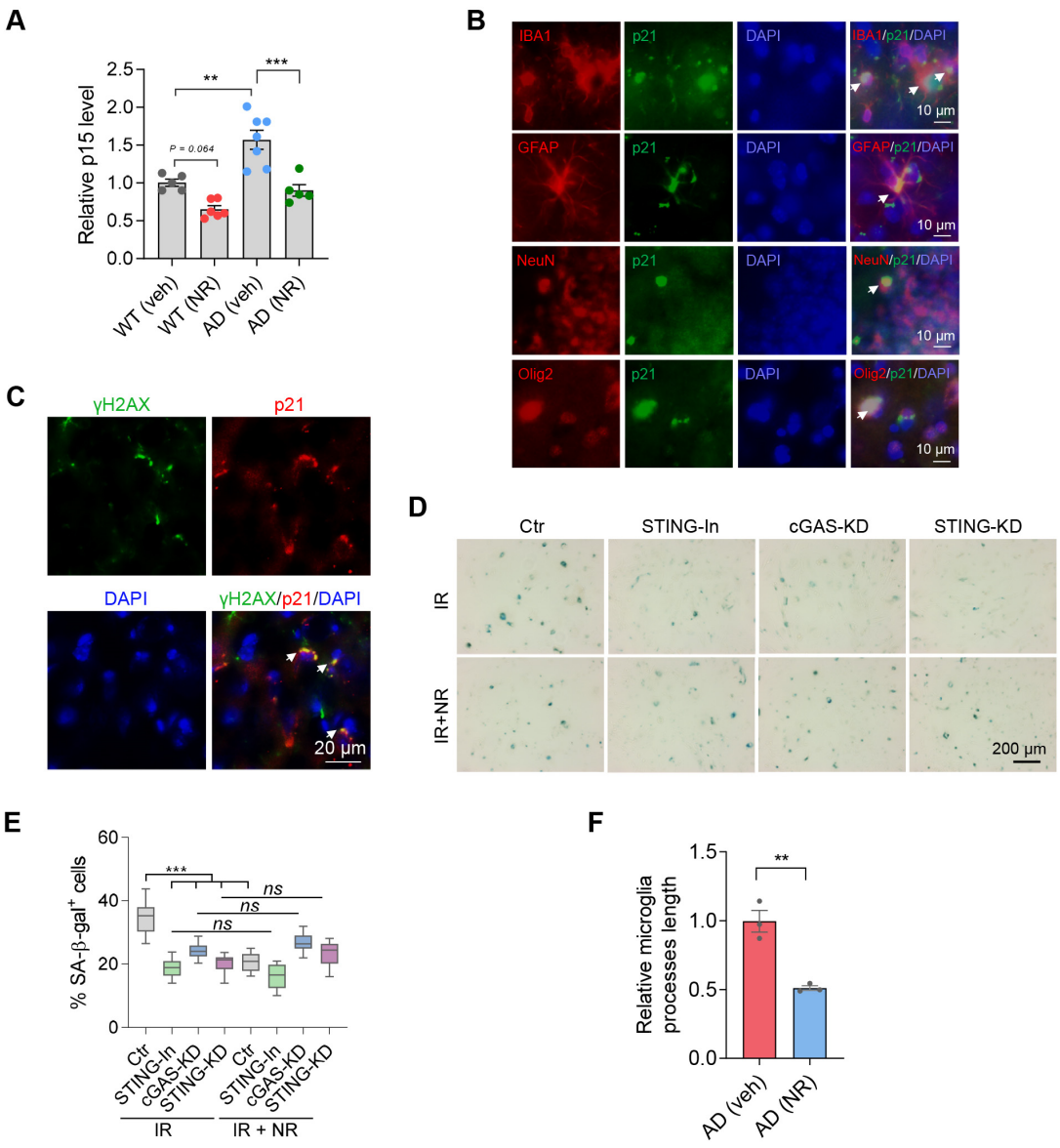

Fig. S6. NR decreases cellular senescence through the cGAS–STING pathway and improves microglia phagocytosis.
(**A**) Quantitative real-time PCR of relative p15 mRNA levels. n = 5-7 mice per group. (**B**) Immunofluorescence of microglia marker IBA1 or astrocyte marker GFAP or neuron marker NeuN or oligodendrocyte progenitor cell marker Olig2 with cellular senescence marker p21 in AD mouse brains. White arrows point to colocalization. (**C**) Immunostaining of DNA damage marker γH2AX with cellular senescence marker p21 in AD mouse brain sections. White arrows showed their colocalization. (**D**) Representative SA-β-gal staining in IR-treated HMC3 microglia cells. Cells were treated with STING inhibitor or cGAS siRNA or STING siRNA to investigate NR function of decreasing senescence in cGAS–STING knockdown HMC3 cells. IR dose: one time 3 Gy. Cells were then cultured (with NR or vehicle) for another 9 days. (**E**) Quantification of SA-β-gal positive cells in Supplementary Fig. S6D. n = 18 pictures per group. (**F**) Quantification of microglia processes length in NR- or vehicle- treated NR mice brains (related to Fig. 6A). n = 3 mice per group. Data: mean ± S.E.M. Statistical significance was performed with Student's *t*-test or two-way ANOVA followed by Tukey's multiple comparisons test. * $P < 0.05$, ** $P < 0.01$, *** $P < 0.001$.

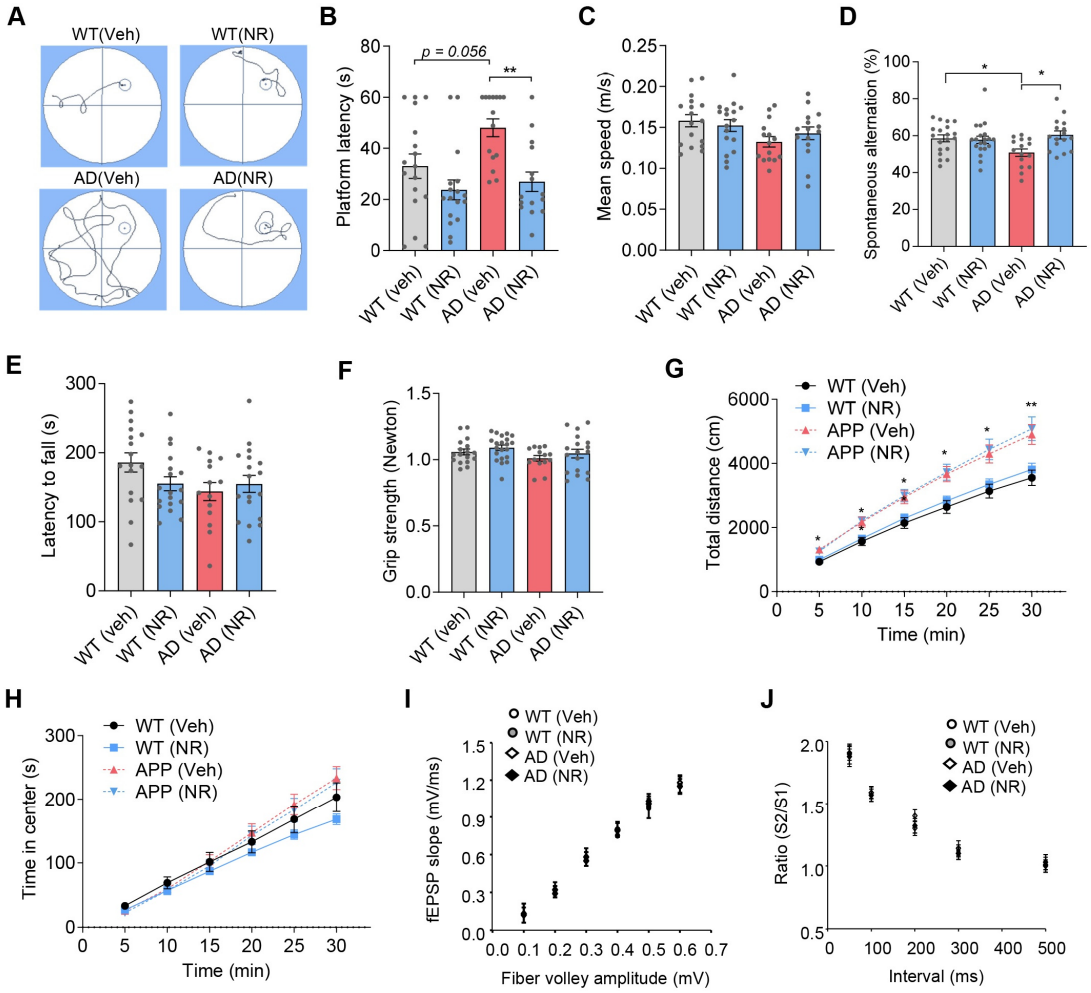

Fig. S7. NR improves memory ability in AD mice.
(**A**) Representative mice swimming paths on the last training day of Morris water maze. (**B**) The latency to find the platform during probe trial in Morris water maze test. (**C**) The mean swimming speed during probe trial in Morris water maze test. n = 15-17 mice per group. (**D**) Spontaneous alternation in the Y-maze test. n = 15-19 mice per group. (**E**) The latency to first fall in the rotarod test. n = 14-18 mice per group. (**F**) The grip strength (newton) in grip strength test. n = 14-21 mice per group. (**G**) The total distance in the open field test. (**H**) The time in center zone in the open field test. for G-H, n = 18-21 mice per group. (**I**) Input–output curves in which the postsynaptic responses (fEPSP) are plotted as a function of increasing intensity of presynaptic stimulation (fiber volley amplitude). (**J**) Results of paired-pulse facilitation analysis, a measure of excitatory neurotransmitter (glutamate) release from presynaptic terminals. For I-J, values are the mean and SEM of determinations made on eight hippocampal slices from at least five different mice. Data: mean ± S.E.M. Statistical significance was performed with two-way ANOVA followed by Tukey multiple comparisons test. * $P < 0.05$, ** $P < 0.01$, *** $P < 0.001$.

SI References

1. C. V. Vorhees, M. T. Williams, Morris water maze: procedures for assessing spatial and related forms of learning and memory. *Nat Protoc* **1**, 848-858 (2006).
2. Y. Hou *et al.*, NAD(+) supplementation normalizes key Alzheimer's features and DNA damage responses in a new AD mouse model with introduced DNA repair deficiency. *Proc. Natl. Acad. Sci. U. S. A.* **115**, E1876-E1885 (2018).
3. E. F. Fang *et al.*, Mitophagy inhibits amyloid-beta and tau pathology and reverses cognitive deficits in models of Alzheimer's disease. *Nat. Neurosci.* **22**, 401-412 (2019).
4. K. Ghosal *et al.*, Alzheimer's disease-like pathological features in transgenic mice expressing the APP intracellular domain. *Proc Natl Acad Sci U S A* **106**, 18367-18372 (2009).
5. M. Kritsilis *et al.*, Ageing, Cellular Senescence and Neurodegenerative Disease. *Int. J. Mol. Sci.* **19** (2018).
6. A. Cheng *et al.*, Mitochondrial SIRT3 Mediates Adaptive Responses of Neurons to Exercise and Metabolic and Excitatory Challenges. *Cell Metab* **23**, 128-142 (2016).
7. J. L. Jankowsky *et al.*, Co-expression of multiple transgenes in mouse CNS: a comparison of strategies. *Biomol. Eng.* **17**, 157-165 (2001).
8. M. Scheibye-Knudsen *et al.*, A high-fat diet and NAD(+) activate Sirt1 to rescue premature aging in cockayne syndrome. *Cell Metab* **20**, 840-855 (2014).
9. J. Zhang *et al.*, The AAA+ ATPase Thorase regulates AMPA receptor-dependent synaptic plasticity and behavior. *Cell* **145**, 284-299 (2011).
10. H. F. Iaccarino *et al.*, Gamma frequency entrainment attenuates amyloid load and modifies microglia. *Nature* **540**, 230-235 (2016).
11. L. D. Aarreberg *et al.*, Interleukin-1beta Induces mtDNA Release to Activate Innate Immune Signaling via cGAS-STING. *Mol. Cell* **74**, 801-815 e806 (2019).